Proceedings of the 10o Brazilian Congress of Thermal Sciences and Engineering -- ENCIT 2004
Braz. Soc. of Mechanical Sciences and Engineering -- ABCM, Rio de Janeiro, Brazil, Nov. 29 -- Dec. 03, 2004

LAMINAR NATURAL CONVECTION IN A SQUARE ENCLOSURE WITH AN INTERNAL ROTATING HEATED CYLINDER

Paulo Mohallem Guimarães
Universidade Federal de Itajubá – UNIFEI
Departamento de Engenharia Mecânica
Avenida BPS, 1303 – Pinheirinho – Itajubá – MG – 37500-176
paulomgui@uol.com.br

Doacir Vilar de Assis Junior
Universidade Federal de Itajubá – UNIFEI
Departamento de Engenharia Mecânica
Avenida BPS, 1303 – Pinheirinho – Itajubá – MG – 37500-176
doajunior@yahoo.com.br

Genésio José Menon
Universidade Federal de Itajubá – UNIFEI
Departamento de Engenharia Mecânica
Avenida BPS, 1303 – Pinheirinho – Itajubá – MG – 37500-176
genesio@iem.unifei.com.br

Abstract. *It is studied in this work the behavior of the natural convection heat transfer and the velocity distribution inside an enclosure with an internal heated rotating cylinder. The Reynolds number as well as the Grashof number are respectively varied as follows: $1 \leq Re \leq 500$ and $10^3 \leq Gr \leq 10^5$. The effect of the inclinaton angle is also taken into consideration $\gamma = 45°$. The Petrov-Galerkin method together with the Penalty formulation are used to solve the governing equations. In general, it is noted a better heat transfer for the cylinder rotating in the counterclockwise direction. The internal cylinder angular velocities contribute to enhance or decrease the Nusselt number by also bringing up recirculations that inhibit flow or enhancement of the buoyancy-induced flow.*

Keywords: finite element method, rotating cylinder, Petrov-Galerkin, convective heat transfer, laminar flow

1. Introdução

The study of natural convection in an enclosure has been carried out for decades due to its importance in engineering applications such as solar energy systems, electronic cooling equipment, etc.

In Fu et al. (1994), a penalty finite-element numerical method is used to investigate enhancement of natural convection of an enclosure by a rotating circular cylinder near a hot wall. They conclude that the direction of the rotating cylinder plays a role in enhancing natural convection in an enclosure. In this study, the counter-clockwise rotating cylinder apparently contributes to the heat transfer rate, but the clockwise rotating cylinder does not. When the value of the Richardson number is about 10^3, the enhancement of the heat transfer rate begins to be revealed. The maximum enhancement of the heat transfer is approximately equal to 60%.

Nguyen et al. (1996) investigate numerically the heat transfer from a rotating circular cylinder immersed in a spatially uniform, time-dependent convective environment including the effects due to buoyancy force. The flow equations, based on the vorticity and stream function, are solved along with the energy equation by a hybrid spectral scheme that combines the Fourier spectral method in the angular direction and a spectral element method in the radial direction. Several cases are simulated for Grashof numbers up to 2×10^4, Reynolds numbers up to 200, and a range of speed of rotation from –0.5 to +0.5. The results show that vortex shedding is promoted by the cylinder rotation but is vanished by the presence of the buoyancy force. In opposing flows, the counter flow currents cause a large expansion of the streamlines and isotherms in the direction normal to the free stream velocity. These changes in the structure of the flow and the temperature fields greatly modify the heat flux along the surface of the cylinder and consequently, the heat transfer rate is strongly dependent upon Reynolds number, Grashof number, rotational speed, and the gravity direction. Effects due to pulsation are also reflected in the Nusselt number history in the form of periodic oscillations.

Lee et al. make experimental investigations to study the convective phenomena of an initially stratified salt-water solution due to bottom heating in a uniformly rotating cylindrical cavity. Three types of global flow patterns initially appear depending on the effective Rayleigh number and Taylor number: stagnant flow regime, single mixed layer flow regime and multiple mixed layer flow regime. The number of layers at its initial stage and the growth height of the mixed layer decreases for the same Rayleigh number. It is ascertained in the rotating case that the fluctuation of interface between layers is weakened, the growth rate of mixed layer is retarded and the shape of interface is moire regular compared to the stationary case.

Joo-Sik Yoo (1998) studies numerically the mixed convection in a horizontal concentric annulus with Prandtl number equal to 0.7. The inner cylinder is hotter than the outer cylinder. The forced flow is induced by the cold outer

cylinder that rotates slowly with constant angular velocity with its axis at he center of the annulus. Investigations are made for various combinations of Rayleigh number Ra, Reynolds number Re, and ratio σ of the inner cylinder diameter to the gap width, that is, $Ra \leq 5 \times 10^4$, $Re \leq 1500$, and $0.5 \leq \sigma \leq 5$. The flow patterns can be categorized into three types according to the number of eddies: two-one- and no-eddy flows. The transitional Reynolds number between two-and one-eddy flows for small Rayleigh number is not greatly affected by the geometrical parameter σ. Net circulation of fluid in the direction of cylinder's rotation is decreased as Ra is increased. As the speed of the cylinder's rotation is increased, the points of maximum and minimum local heat fluxes at both of the inner and outer cylinders move in the same direction of cylinder's rotation for small Ra, but for high Ra the points at the inner cylinder do not always move in the same direction. Overall heat transfer at the wall is rapidly decreased, as Re approaches the transitional Re between two- and one-eddy flows.

Lin and Yan (2000) conducted an experimental study through temperature measurements to investigate the thermal features induced by the interaction between the thermal buoyancy and rotation-induced Coriolis force and centrifugal force in an air-filled heated inclined cylinder rotating about its axis. Results are obtained ranging the thermal Rayleigh number, the Taylor number, the rotational Rayleigh number, and the inclined angle. The experimental data suggest that when the cylinder is stationary, the thermal buoyancy driven flow is random oscillation at small amplitude after initial transient for inclined angle smaller than 60°. Rotating the cylinder is found to destabilize the temperature field when the rotation speed is less than 30 rpm and to stabilize it when the rotation speed exceeds 30 rpm. Moreover, the distributions of time-average temperature in the Z-direction for various inclined angles become widely separate only at low rotation rates less than 60 rpm.

2. Problem description

In this work, a natural convection study in a square cavity with an internal heated rotating cylinder is carried out. The cylinder is rotated in two directions – clockwise and counterclockwise. Figure 1 shows the geometry and the boundary conditons of the problem. It is a square cavity with height L, width W, and an internal cylinder with radius r_0. The side walls are isothermally cooled Tc and heated Th. The horizontal walls with respect to the x-direction are kept isolated. The internal cylinder surface is hot with temperature Th and rotates with an angular velocity ω. The Nusselt numbers, the isotherms, the velocity vectors will be analysed by ranging the Reynolds number, the Grashof number, and the inclination of the cavity.

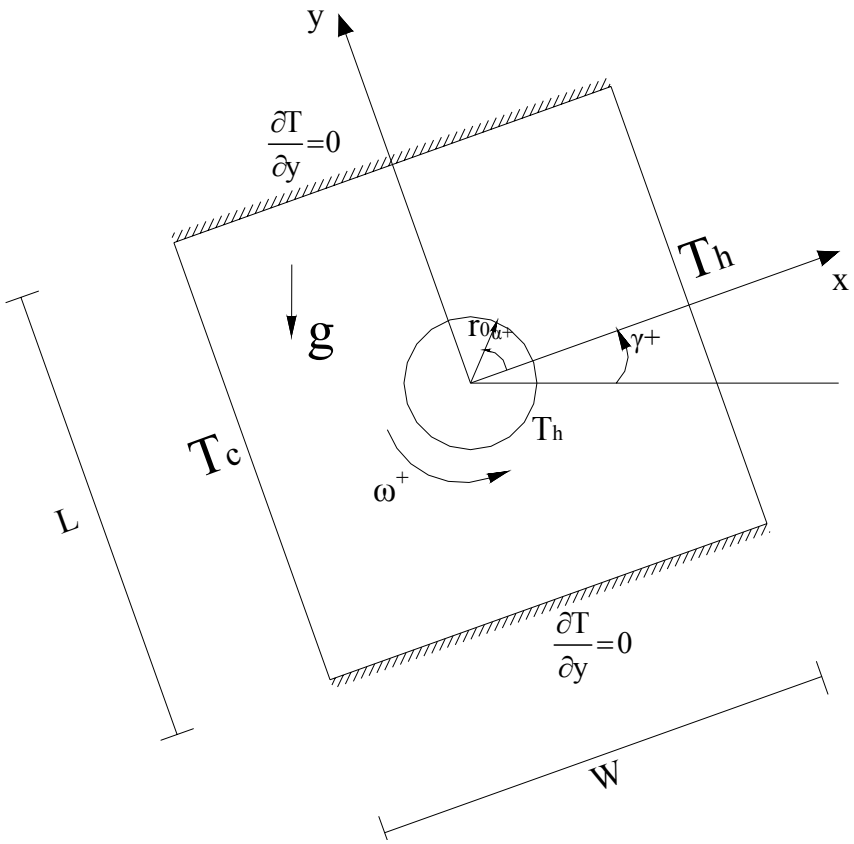

Figure 1. Geometry and boundary conditions of the problem.

3. Problem formulation

The problem governing equations are given by the equations of mass conservation, Navier-Stokes, and energy. Being that u and v are the velocity components, T is the fluid temperature, t' is the time field, D_T is the thermal diffusivity, β_T is the thermal expansion coefficient, ν is the kinematic viscosity, *g* is the gravitational acceleration, ρ_0 is the fluid density and T_0 is the reference temperature taken as $T_0 = T_c$.

Under the Boussinesq approximation and the following dimensionless parameters:

$$X=\frac{x}{L};\ Y=\frac{y}{L};\ U=\frac{u}{u_{max}};\ V=\frac{v}{u_{max}};\ P=\frac{p}{\rho_0 u_{max}^2};\ t=\frac{t'}{(L/u_{max})'};\ \theta=(T-T_c)/(T_h-T_c)$$

$$Fr=\frac{Re^2}{Gr};\ Pr=\frac{\nu}{D_T};\ Gr=\frac{\beta_T g\Delta T L^3}{\nu^2};\ Re=\frac{u_{max}\rho_0 2r_0}{\mu};\ \Delta T=T_h-T_c\ ;\ A_r=\frac{L}{2r_0} \tag{1}$$

where Fr, Pr, Gr, Re, u_{max}, A_r and μ are, respectively, the Froude number, the Prandtl number, the Grashof number, the Reynolds number, the velocity $(r_0\,\omega)$, the aspect ratio, and the dynamic viscosity, the dimensionless governing equations can be cast into the following form:

$$\frac{\partial U}{\partial X}+\frac{\partial V}{\partial Y}=0; \tag{2}$$

$$\frac{\partial U}{\partial t}+U\frac{\partial U}{\partial X}+V\frac{\partial U}{\partial Y}=-\frac{\partial P}{\partial X}+\frac{1}{Re}\left(\frac{\partial^2 U}{\partial X^2}+\frac{\partial^2 U}{\partial Y^2}\right)\frac{1}{A_r}+\sin(\gamma)\frac{\theta}{Fr}\frac{1}{A_r^2}; \tag{3}$$

$$\frac{\partial V}{\partial t}+U\frac{\partial V}{\partial X}+V\frac{\partial V}{\partial Y}=-\frac{\partial P}{\partial Y}+\frac{1}{Re}\left(\frac{\partial^2 V}{\partial X^2}+\frac{\partial^2 V}{\partial Y^2}\right)\frac{1}{A_r}+\cos(\gamma)\frac{\theta}{Fr}\frac{1}{A_r^2}; \tag{4}$$

$$\frac{\partial \theta}{\partial t}+U\frac{\partial \theta}{\partial X}+V\frac{\partial \theta}{\partial Y}=\frac{1}{Re\,Pr}\left(\frac{\partial^2 \theta}{\partial X^2}+\frac{\partial^2 \theta}{\partial Y^2}\right)\frac{1}{A_r}. \tag{5}$$

The boundary conditions are as follows:

$X = 0, U = V = 0, \theta = 0$,
$X = 1, U = V = 0, \theta = 1$,
$Y = 0, U = V = 0, \frac{\partial \theta}{\partial Y} = 0$,
$Y = 1, U = V = 0, \frac{\partial \theta}{\partial Y} = 0$.

On the cylinder surface:

$\theta = 1$, $U = \pm \sin\alpha$, $V = \pm \cos\alpha$.

The sign "+" or "-" depends on the rotating direction of the cylinder.
The average Nusselt number along a surface S can be written as:

$$Nu = \frac{1}{S}\int_S \frac{\partial \theta}{\partial n}\, ds.$$

where n means the direction perpendicular to the surface S which can be the hot, cold, or cylinder surface.

4. The solution method

By applying the Petrov-Galerkin formulation to the equations above, Eqs. (2) to (5), together with the Penalty technique , the weak form of the conservation equations is as follows:

$$\int_\Omega N_i\left[\frac{\partial U}{\partial t}+\frac{1}{Re}\left(\frac{\partial N_i}{\partial X}\frac{\partial U}{\partial X}+\frac{\partial N_i}{\partial Y}\frac{\partial U}{\partial Y}\right)\frac{1}{A_r}\right]d\Omega+\int_\Omega^R \lambda\frac{\partial N_i}{\partial X}\left(\frac{\partial U}{\partial X}+\frac{\partial V}{\partial Y}\right)d\Omega= \int_\Omega\left[\left(N_i+P_{il}\right)\left(U\frac{\partial U}{\partial X}+V\frac{\partial U}{\partial Y}\right)+N_i\sin(\gamma)\frac{\theta}{Fr}\frac{1}{A_r^2}\right]d\Omega-\int_{\Gamma_0}N_i\,p\,n_x\,d\Gamma \tag{6}$$

$$\int_\Omega N_i\left[\frac{\partial V}{\partial t}+\frac{1}{Re}\left(\frac{\partial N_i}{\partial X}\frac{\partial V}{\partial X}+\frac{\partial N_i}{\partial Y}\frac{\partial V}{\partial Y}\right)\frac{1}{A_r}\right]d\Omega+\int_\Omega^R \lambda\frac{\partial N_i}{\partial Y}\left(\frac{\partial U}{\partial X}+\frac{\partial V}{\partial Y}\right)d\Omega= \int_\Omega\left[\left(N_i+P_{il}\right)\left(U\frac{\partial V}{\partial X}+V\frac{\partial V}{\partial Y}\right)+N_i\cos(\gamma)\frac{\theta}{Fr}\frac{1}{A_r^2}\right]d\Omega-\int_{\Gamma_0}N_i\,p\,n_y\,d\Gamma \tag{7}$$

$$\int_\Omega\left[N_i\frac{\partial\theta}{\partial t}+\frac{1}{Re\,Pr}\left(\frac{\partial N_i}{\partial X}\frac{\partial\theta}{\partial X}+\frac{\partial N_i}{\partial Y}\frac{\partial\theta}{\partial Y}\right)\frac{1}{A_r}\right]d\Omega=\int_\Omega\left(N_i+P_{i2}\right)\left(U\frac{\partial\theta}{\partial X}+V\frac{\partial\theta}{\partial Y}\right)d\Omega \tag{8}$$

where q = 0 (no heat flux). The dependent variables are approximated by:

$$\Phi(X,Y,t)=\sum_j N_j(X,Y)\Phi_j(t)\;;\; p(X,Y,t)=\sum_k M_k(X,Y)p_k(t). \tag{9}$$

N_i and N_j denote the linear shape functions for Φ, that is, for U, V, and θ, and M_k denote the shape functions for the constant piecewise pressure. P_{ij} are the Petrov-Galerkin perturbations applied to the convective terms only. The terms P_{ij} are defined as follows:

$$P_{ij}=k_j\left(U\frac{\partial N_i}{\partial X}+V\frac{\partial N_i}{\partial Y}\right);\; k_j=\frac{\alpha_j\bar{h}}{|V|};\; \alpha_j=\coth\frac{\gamma_j}{2}-\frac{2}{\gamma_j};\; \gamma_j=\frac{|V|\bar{h}}{\varepsilon_j};\; j=1,2 \tag{10}$$

where γ is the element Péclet number, $|V|$ is the absolute value of the velocity vector that represents the fluid average velocity within each element, $\bar{h}$ is the element average size, $\varepsilon_1=1/Re\,A_r, \varepsilon_2=1/Pe\,A_r$, and λ is the Penalty parameter which is considered to be 10^9. The time integration is by a semi-implicit backward Euler method. Moreover, the convective terms are calculated explicitly and the viscous and Penalty terms implicitly. The temperatures and velocities are interpolated by using the four-node quadrilateral elements and the pressure by the one-node ones. Finally, the reduced integration is applied to the penalty term to avoid numerical locking.

The algorithm is extensively validated by comparing the results of the present work with both the ones obtained in experimental and numerical investigations. Figures (2) and (3) show the geometries and the boundary conditions used in the first and second comparisons, respectively.

The first comparison is accomplished not only by using the experimental results presented by Lee and Mateescu (1998) and Armaly (1983) et al., but also by the numerical ones achieved by Lee and Mateescu (1998), Gartling (1990), Kim and Moin (1985), and Sohn (1988). The air flow of the present comparison analysis is taken as bidimensional, laminar, incompressible, and under the unsteady regime. The domain is a horizontal upstream backward-facing step channel whose inlet has a fully developed velocity profile given by u = 24y(0.5-y) $\overline{U}$ and v = 0 in which Re = 800. The computational domain is shown in Fig. (2) where all walls are under the no-slip condition.

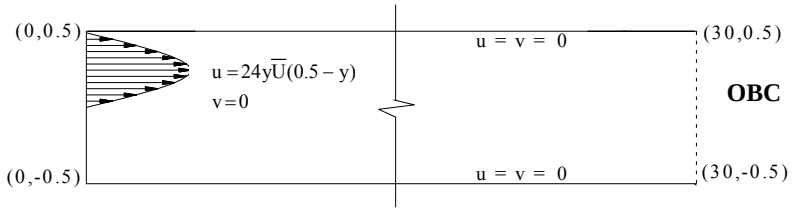

Figure 2. Geometry and boundary conditions for the first comparison.

Table (1) shows the results from the first comparison for the flow separation distance Xs on the upper surface and its reattachment distance Xrs. As for the bottom surface, the comparison is made on the reattachment distance Xr. As it can be noticed, the results of the present work agree well with the ones from the literature.

Table1. Comparison of computed predictions and experimental measurements of dimensionless lengths (with respect to the channel height) of separation and reattachment on upper and lower walls.

		Experimental results			Computed results			
	Length on	Lee and Mateescu (1998)	Armaly et al. (1983)	Present prediction	Gartling´s prediction (1990)	Kim & Moin (1985)	Lee and Mateescu (1998)	Sohn (1988)
Lower Wall	x_r	6.45	7.0	5.75	6.1	6.0	6.0	5.8
Upper Wall	x_s	5.15	5.7	4.95	4.85	-	4.8	-
	x_{rs}	10.25	10.0	9.9	10.48	-	10.3	-
	x_{rs}-x_s	5.1	4.3	4.95	5.63	5.75	5.5	4.63
Reynolds		805	800	800	800	800	800	800
Hd/Hu		2	1.94	2	2	2	2	2

The second comparison is performed with the numerical results shown by Comini (1997) et all. The contrasting study is carried out by considering a problem involving mixed convective heat transfer with the flow being bidimensional, laminar, and incompressible in the unsteady

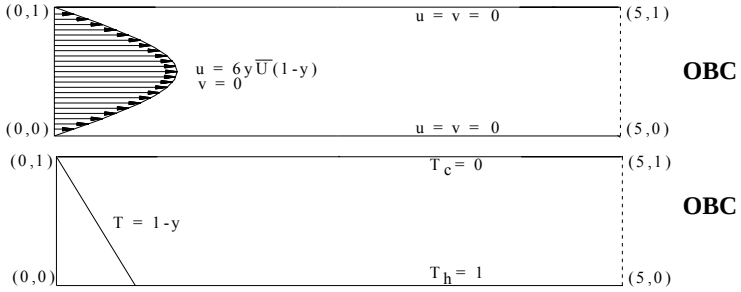

Figure 3. Geometry and boundary conditions for the second comparison.

regime. In this case, some values are chosen such as Re=10, Pr = 0.67, and Fr = 1/150. The grid has 4000 quadrilateral four-noded elements with $\Delta x = 0.1$, $\Delta y = 0.15$, $\Delta t = 0.01$ and 1000 iterations. Figure (4) displays the average Nusselt number on the upper surface versus time. After approximately iteration 500, the regime turns to be periodic with the average Nusselt number on the upper wall oscillating around a mean value of 2.44. This value agrees satisfactorily with the one found by Comini (1997) et al. which is 2.34, resulting in a deviation of about 4%.

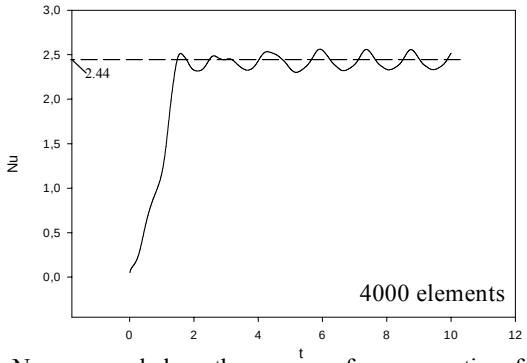

Figure 4. Average Nusselt number Nu measured along the upper surface versus time for a Poiseuille flow heated from below.

Figure 5 pictures the third case studied to validate the mathematical modeling code. The mixed convection of air between two horizontal concentric cylinders with a cooled rotating outer cylinder is analyzed for Prandtl number Pr = 0.7, Re = 10, 50, 100, 150, 200, 250, 300, 350, and 500, and Rayleigh number Ra = 10^4, 2 x 10^4, and 5 x 10^4. The domain is discretized spatially with 5976 non-structured four-node quadrilateral elements.

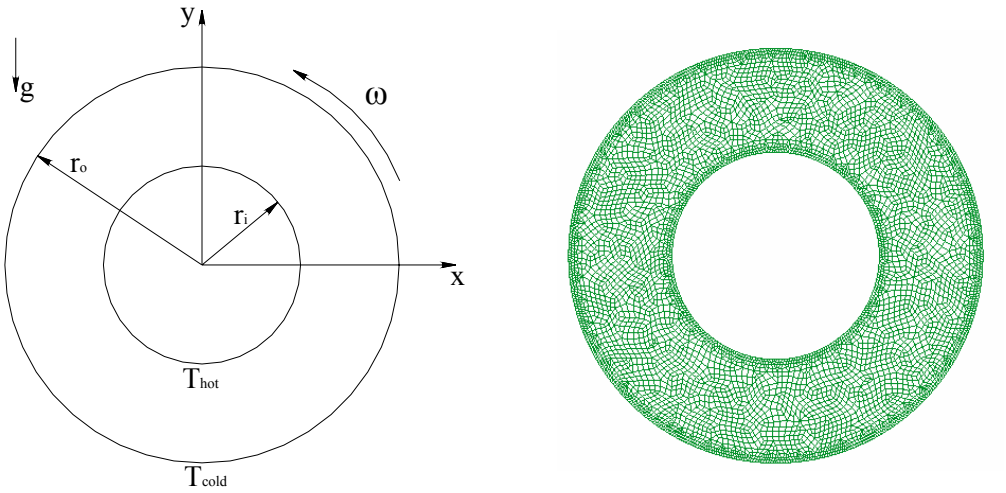

Figure 5. Comparison case: a) Geometry and boundary conditions b) mesh with 5976 elements.

Table 2 shows the Nusselt numbers on the inner cylinder (NUCYLIN) and outer cylinder (NUCYLOUT) surfaces as well as the average Nusselt number (NUMED) of (NUCYLIN) and (NUCYLOUT). These values are compared to the ones found in Yoo (1998). There, different grids are used: meshes of (65X64), (45 x 64), or (65 x 32) for a finite difference scheme. In fact, the results found here are higher than the ones in Yoo(1998), but still with a good agreement. This difference is likely due to different methods and different meshes. The time step used is 0.01 for almost all cases and the number of iterations ranging from 10^4 to $3x10^4$.

Table 2. Values of Nusselt number for concentric cylinders with a mesh of 5976 elements.

Rayleigh	Reynolds	Froud	Peclet	NUCYLIN	NUCYLOUT	NUMED
10000	50	0,175	35	2,6000	1,3221	1,9611
10000	100	0,7	70	2,5622	1,3029	1,9326
10000	150	1,575	105	2,4538	1,2506	1,8522
10000	200	2,8	140	2,2697	1,1598	1,7147
10000	250	4,375	175	2,0386	1,0426	1,5406
10000	300	6,3	210	1,6269	0,8364	1,2317
10000	350	8,575	245	1,4824	0,7629	1,1227
10000	500	17,5	350	1,4374	0,7409	1,0892
20000	100	0,35	70	3,1361	1,5964	2,3662
20000	150	0,7875	105	3,0715	1,5645	2,3180
20000	200	1,4	140	2,9515	1,5051	2,2283
20000	250	2,1875	175	2,7821	1,4204	2,1013
20000	300	3,15	210	2,5824	1,3206	1,9515
20000	350	4,2875	245	2,3793	1,2168	1,7980
20000	500	8,75	350	1,7730	0,9109	1,3420
50000	100	0,14	70	3,9867	2,0324	3,0095
50000	150	0,315	105	3,9587	2,0193	2,9890
50000	200	0,56	140	3,8806	1,9798	2,9302
50000	250	0,875	175	3,7695	1,9234	2,8465
50000	300	1,26	210	3,6443	1,8616	2,7530
50000	350	1,715	245	3,5035	1,7931	2,6483
50000	500	3,5	350	3,0044	1,5373	2,2708

The sensibility of mesh change is analyzed considering three non-structured meshes shown in Fig. 6 as follows:

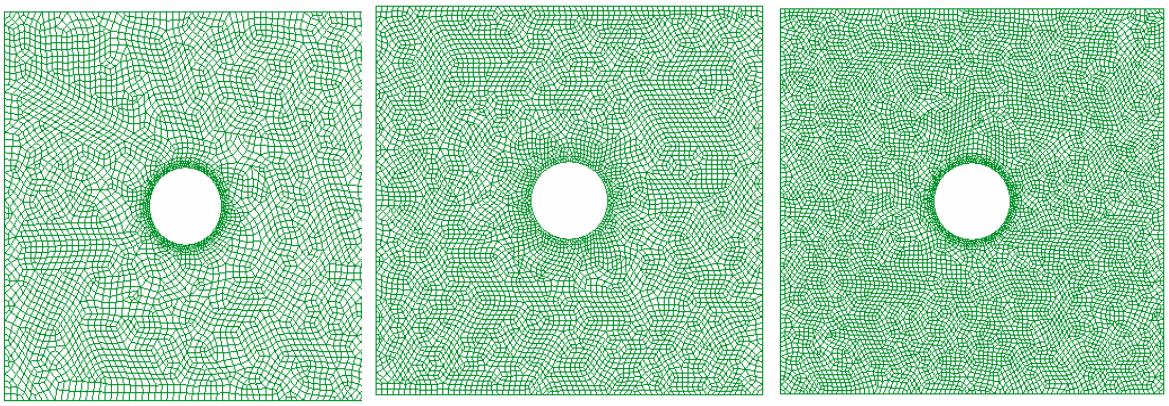

4354 elements 6046 elements 8144 elements

Figure 6. Three meshes used for mesh sensibility study.

Table 3 shows the Nusselt numbers on the cold (NUCOLD), hot (NUHOT), and cylinder (NUCYL) surfaces for $Gr = 10^5$ and Reynolds numbers equal to 1, 10, 100, and 1000 for meshes in Fig. 6. The two opposite rotating directions are also considered for the cylinder surface. As one can see, as the number of elements increases, the deviations tend to decrease. The minimum deviation of the average Nusselt number is of 0.006% for the case where Reynolds number Re = 100 on the internal cylinder rotating counterclockwise in the mesh with 8144 elements. The highest one is found to be 8.4% for the 6046-element mesh on the cold surface considering the clockwise direction. In general, it can be noted a very good agreement not only when clockwise rotating cylinder is concerned but also for the opposite rotating direction. The mesh with 8144 elemenst is chosen for all cases in this work.

Table 3. Deviations for meshes with 4354, 6046, and 8144 elements and $Gr = 10^5$.

Clockwise - CWR									
	4354 elements			**6046 elements**			**8144 elements**		
Re	**NUCOLD**	**NUHOT**	**NUCYIL**	**NUCOLD**	**NUHOT**	**NUCYIL**	**NUCOLD**	**NUHOT**	**NUCYIL**
1	5.7776	2.7676	4.1315	5.6246 (2.6%)	2.8326 (2.4%)	4.2351 (2.5%)	5.5367 (1.6%)	2.8317 (0.03%)	4.2711 (0.9%)
10	5.7943	2.7754	4.1552	5.6518 (2.5%)	2.8423 (2.4%)	4.2602 (2.5%)	5.5589 (1.6%)	2.8414 (0.03%)	4.2999 (0.9%)
100	5.3126	2.6429	3.6425	5.1827 (2.5%)	2.7183 (2.9%)	3.7135 (1.9%)	5.0839 (1.9%)	2.7148 (0.1%)	3.7524 (1%)
1000	3.5262	1.5343	2.8640	3.2291 (8.4%)	1.4501 (5.5%)	2.6952 (5.9%)	3.1447 (2.6%)	1.44 (0.7%)	2.8435 (5.5%)
Counterclockwise - CCWR									
1	5.7705	2.7647	4.1225	5.6149 (2.7%)	2.8293 (2.3%)	4.2254 (2.5%)	5.5281 (1.6%)	2.8285 (0.03%)	4.2607 (0.8%)
10	5.7236	2.7483	4.0641	5.5560 (2.9%)	2.8116 (2.3%)	4.1620 (2.4%)	5.4746 (1.5%)	2.8105 (0.04%)	4.1943 (0.8%)
100	5.1766	2.8585	3.0054	4.9339(4.7%)	2.9360 (2.7%)	3.0039 (0.05%)	4.8711 (1.3%)	2.9362 (0.006%)	3.0542 (1.7%)
1000	5.3368	3.2304	2.7259	5.0144 (6.1%)	3.3066 (2.4%)	2.7023 (0.9%)	4.9917 (0.5%)	3.3266 (0.6%)	2.7510 (1.8%)

5. Results

Figure 7 shows the temperature distributions for Grashof number Gr = 10^5 and inclination angle $\gamma = 0°$ with Reynolds numbers equal to Re = 1, 10, 50, 100, and 500. The isotherms are shown for the two opposite directions. The Reynolds variation is related to the variation of the angular velocity ω of the surface of the internal cylinder. This is due to the definition of the Reynolds number. It can be clearly seen the influence of the rotation of the cylinder on the temperature distributions. Up to Re = 10, no significant change is found. On the other hand, over that point the isotherms tend to be different as Re increases. Interestingly, although for Re = 1, there is hot fluid confined in the upper part of the enclosure, its temperature gradients along the vertical walls and o the cylinder surface change sufficiently to guarantee the highest Nusselt numbers in general. Surprisingly, as Re increases, the overall temperatures tend to increase, hence decreasing the Nusselt numbers.

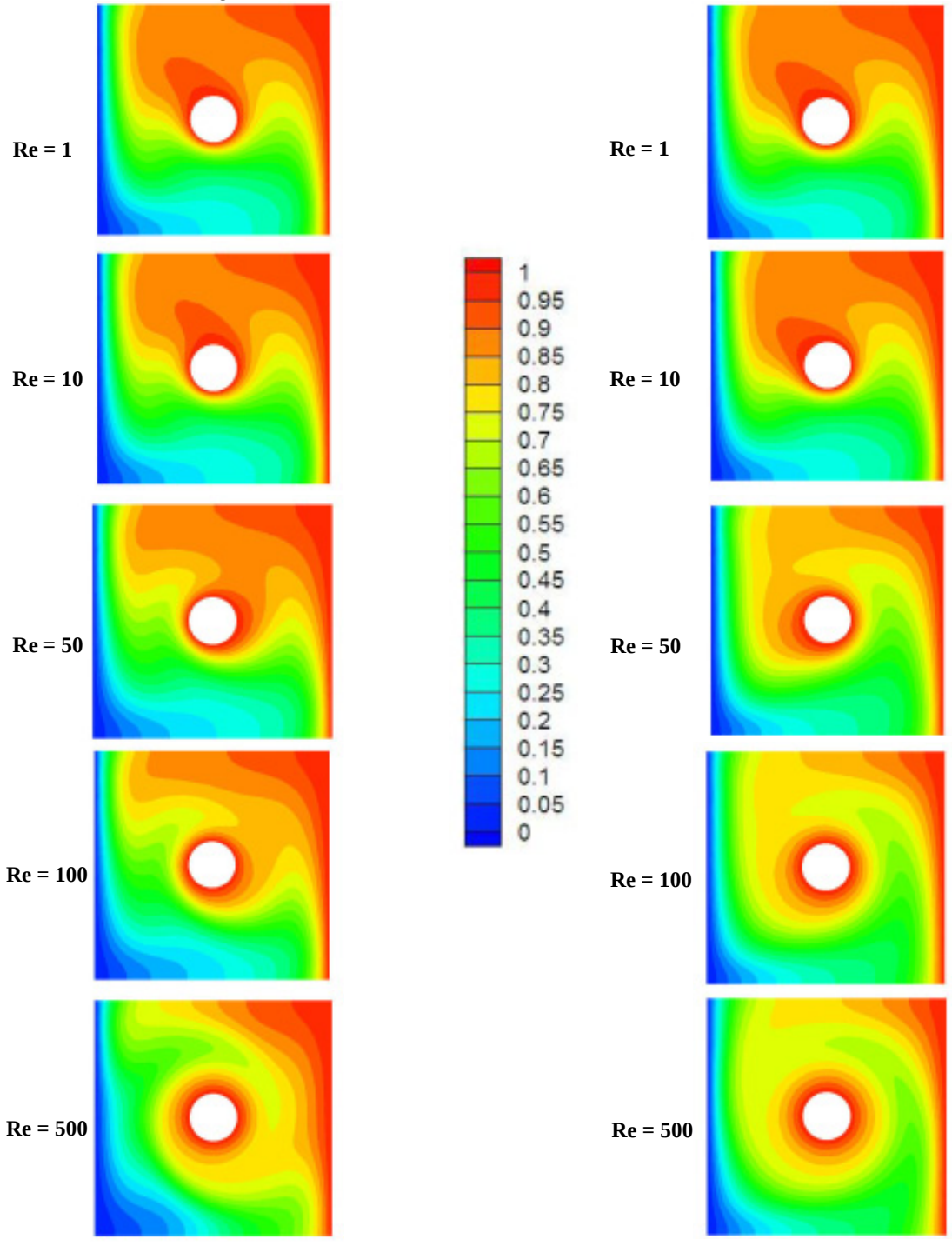

Figure 7. Isotherms for Gr = 10^5 in the clockwise and counterclockwise rotating directions.

It can also be noted that as Re increases, the temperature around the cylinder tends to be stratified. It is worth observing that for Re = 500 and the clockwise direction, the temperature gradient along the hot wall is weak, hence leading to higher temperatures. When cooling is aimed, this is a case that has to be avoided. Although for this case Re = 500, it seems that the fluid is sort of stagnant along the hot wall, then increasing the temperatures near the hot wall so decreasing its Nusselt number.

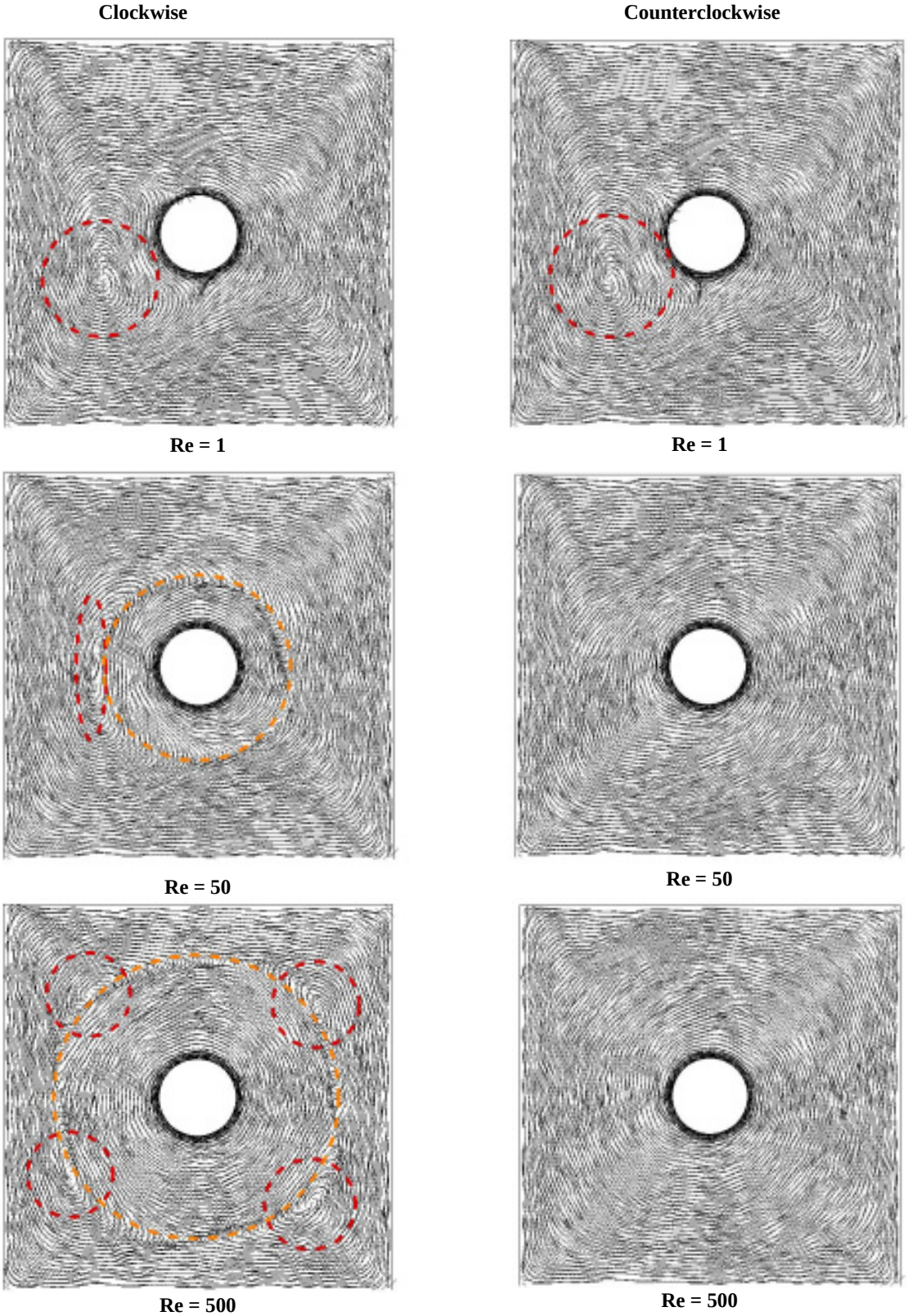

Figure 8. Velocity vectors for Gr = 10^5 and $\gamma = 0°$.

It is depicted in Fig. 8 the velocity vectors for Gr = 10^5, γ = 0°, Re = 1, 50, and 500 in the two opposite rotating cases. It is important to observe that when building the figure, the scale of the vectors was just one in order to keep the figure suitable to be analyzed. In other words, the size of the vectors does not reflect proportionally the size of the magnitude of the velocity fields. However, the way it is disposed is easier to see the recirculations happening inside the enclosure. The yellow dashed lines mean the recirculations and the blue ones mean the separation region of the flow with opposite directions caused by the rotation of the cylinder and the flow risen due to buoyancy forces. As Re increases, the recirculations tend to decrease and the flow around the cylinder tend to be purely a forced flow. The flow presented when Re = 500 with the cylinder in the clockwise direction gives the worst case when cooling is aimed. In a general way, the clockwise rotating cases are the best ones for Gr = 10^5. But this behavior will not be a standard, as it will be shown ahead in this work.

The behavior of the average Nusselt number along the cold wall (NUCOLD), the hot wall (NUHOT), and the cylinder wall (NUCYL) is shown in Fig. 9 in relation to the Reynolds number for Grashof numbers Gr = 10^3, 10^4, and 10^5, and the inclination angle γ = 0°. For Gr = 10^3, it does not seem to appear significant change when considering the opposite directions. However, as Grashof number increases, the counterclockwise cases present higher Nusselt numbers except for Gr = 10^5 as mentioned previously. In a general way, the hot wall is the surface that presents the smallest heat transfer. Just for Gr = 10^5 and Re = 500, the hot wall Nusselt number is higher than the cylinder wall one. Overall, for low Reynolds numbers, the Nusselt distributions do not seem to change when keeping the Grashof number constant. The gradients on the cylinder surface do not change significantly for low Grashof numbers as they do for higher ones.

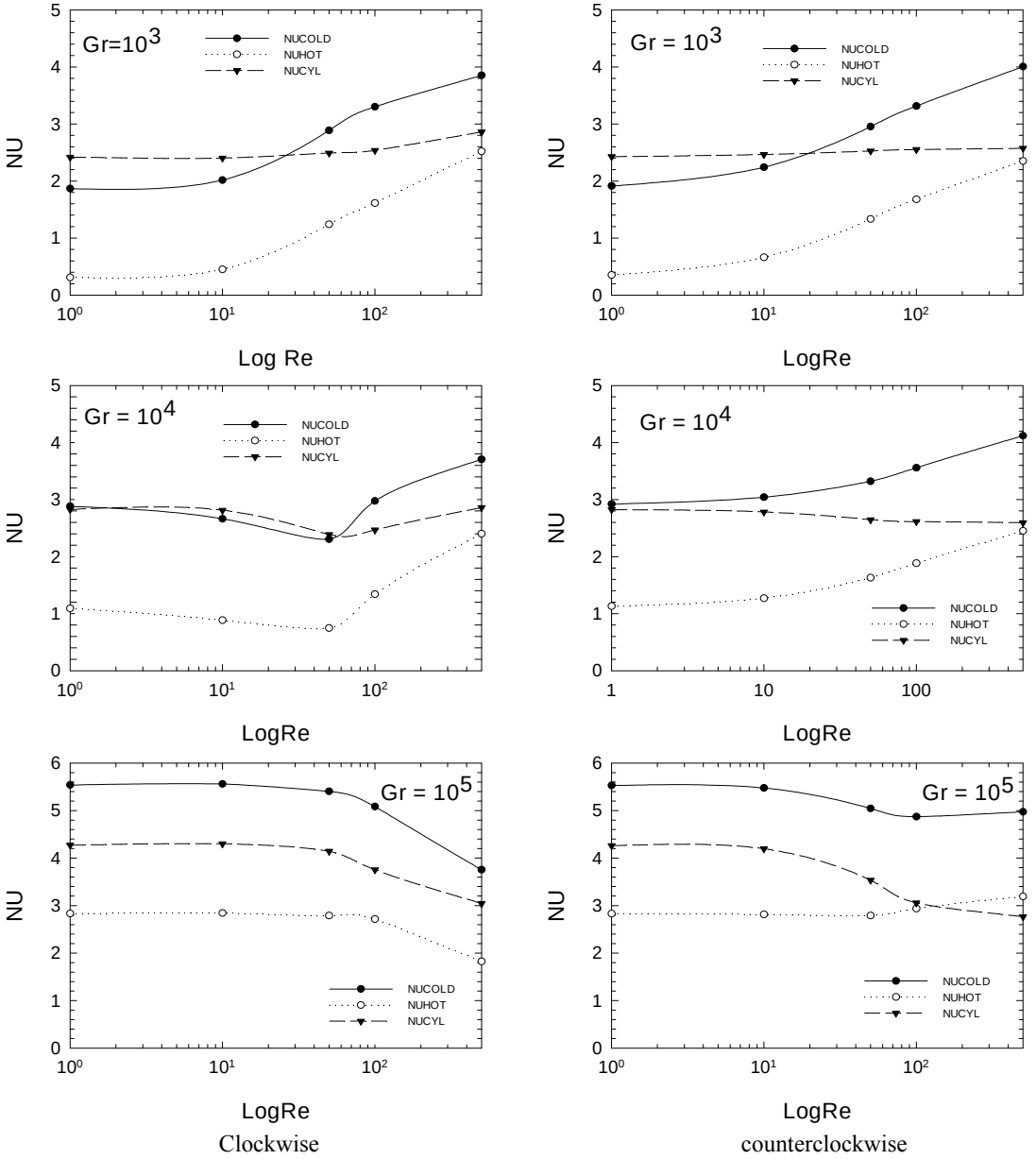

Figure 9. Nusselt versus Reynolds 1 ≤ Re ≤ 500 for Gr = 10^3, 10^4, and 10^5, γ = 0°, clockwise and counterclockwise.

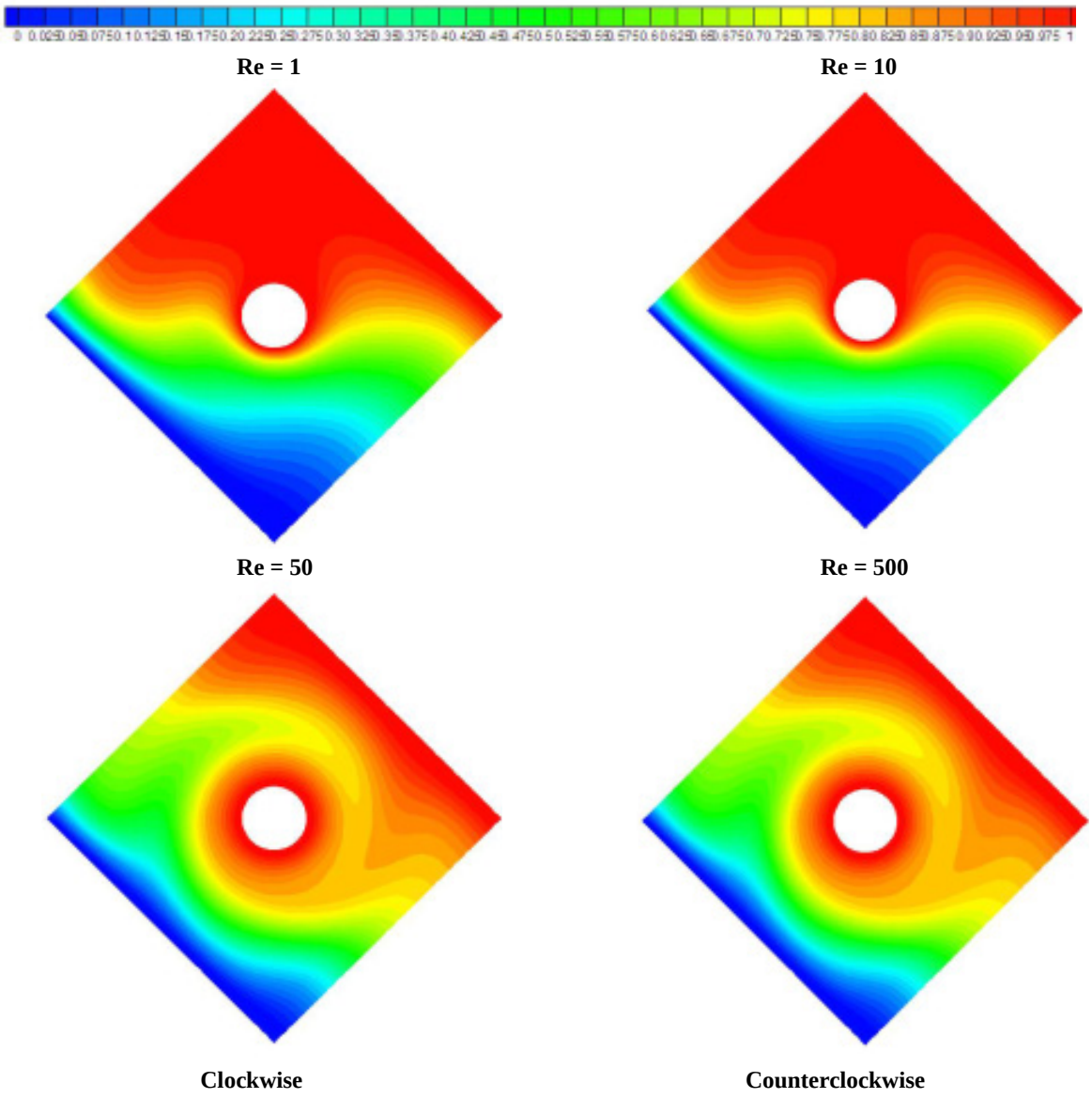

Figure 10. Isotherms for Gr = 10^5 and inclination angle $\gamma = 45°$.

Figure 10 shows the isotherms for the cases where Gr = 10^5, Re = 1, 10, 50, and 500, and the inclination angle $\gamma = 45°$ when the internal cylinder is rotating clockwise. As expected, the hot fluid is stagnant in the upper part of the cavity, thus weakening significantly the heat transfer on all the surfaces in general. Then the counterclockwise rotation of the cavity does not contribute to heat transfer. It is suggested to have further study on the effect of the inclination when rotating the enclosure in the opposite direction, that is, the clockwise direction.

6. Conclusions

The study of natural convection in an enclosure with an internal heated rotating cylinder is carried out. The Navier-Stokes and energy equations are solved using the finite element method with the Petrov-Galerkin technique for the convective terms and the Penalty formulation for the pressure terms. A semi-implicit Euler method is used to advance in time. The four-node quadrilateral element is used to discretize de domain of the problem. Various parameters are ranged to study the problem such as the Reynolds number $1 \leq Re \leq 500$, the Grashof number $10^3 \leq Gr \leq 10^5$, and incliantion angle $\gamma = 45°$. The fluid taken into consideration is air with Prandtl number equal to 0.7. It is observed that the cases with counterclockwise rotation direction produce a better heat transfer rate than the ones with clockwise directions with exception of the cases where $Re < 500$ and Gr = 10^5 clockwise case. The movements of the internal cylinder, clockwise and counterclockwise directions, respectively bring about recirculations and reinforcement of flow inside the enclosure. Definitely, the rotation of the cavity of 45° in the counterclockwise direction significantly weaken the Nusselt number, hence, decreasing the heat transfer.

7. Acknowledgements

The authors acknowledge CAPES and CNPQ for the financial support without which this study would be impossible.

8. References

Armaly, B. F., Durst, F., Pereira, and J. C. F. & Schonung, B., 1983, "Experimental and Theoretical Investigation of Backward-Facing Step Flow", Journal of Fluid Mechanics, Vol. 127, pp. 473-496.

Comini, G., Manzam, M. and Cortella, G., 1997, "Open Boundary Conditions for the Streamfunction-Vorticity Formulation of Unsteady Laminar Convection", Numerical Heat Transfer, Part B, Vol. 31, pp. 217-234.

Fu, W.S., Cheng, C.S. and Shieh, W.J., 1994, "Enhancement of Natural Convection Heat Transfer of an Enclosure by a Rotating Circular Cylinder", Int. J. Heat Mass Transfer, Vol. 37, No. 13, pp. 1885-1897.

Gartling, D. K., 1990, "A Test Problem for Outflow Boundary Conditions – Flow over a Backward-Facing Step", International Journal of Numerical Methods in Fluids, Vol. 11, pp. 953-967.

Kim, J. and Moin, P., 1985, "Application of a Fractional-Step Method to Incompressible Navier-Stokes Equations", Journal of Computational Physics, Vol. 59, pp. 308-323.

Lee, J., Kang, S. H. and Son, Y. S., 1999, "Experimental Study of Double-Diffusive Convection in a Rotating Annulus with Lateral Heating", Int. J. Heat Mass Transfer, Vol. 42, pp. 821-832.

Lee, T. and Mateescu, D., 1998, "Experimental and Numerical Investigation of 2-D Backward-Facing Step Flow", Journal of Fluids and Structures, Vol. 8, pp. 1469-1490.

Lin, D. and Yan, W.M., 2000, "Experimental Study of Unsteady Thermal Convection in Heated Rotating Inclined Cylinders", Int. J. Heat Mass Transfer, Vol. 43, pp. 3359-3370.

Nguyen, H. D., Paik, S. and Douglass, R. W., 1996, "Unsteady Mixed Convection About a Rotating Circular Cylinder with Small Fluctuations in the Free-Stream Velocity", Int. J. Heat Mass Transfer, Vol. 39, No. 3, pp. 511-525.

Sohn, J., 1998, "Evaluation of FIDAP on Some Classical Laminar and Turbulent Benchmarks", International Journal of Numerical Methods in Fluids, Vol. 8, pp. 1469-1490.

Yoo, J., 1998, "Mixed Convection of Air Between Two Horizontal Concentric Cylinders with a Cooled Rotating Outer Cylinder", Int. J. Heat Mass Transfer, Vol.41, No. 2, pp. 293-302.